Atomic quasi-Bragg-diffraction in a magnetic field

Document status and date:
Published: 01/01/2009

Document Version:
Publisher's PDF, also known as Version of Record (includes final page, issue and volume numbers)

Please check the document version of this publication:

• A submitted manuscript is the version of the article upon submission and before peer-review. There can be important differences between the submitted version and the official published version of record. People interested in the research are advised to contact the author for the final version of the publication, or visit the DOI to the publisher's website.
• The final author version and the galley proof are versions of the publication after peer review.
• The final published version features the final layout of the paper including the volume, issue and page numbers.

[Link to publication](#)

Atomic quasi-Bragg-diffraction in a magnetic field

K. F. E. M. Domen, M. A. H. M. Jansen, W. van Dijk, and K. A. H. van Leeuwen[*]

Department of Applied Physics, Eindhoven University of Technology, P.O. Box 513, 5600 MB Eindhoven, The Netherlands
(Received 24 November 2008; published 9 April 2009)

We report on a technique to split an atomic beam coherently with an easily adjustable splitting angle. In our experiment metastable helium atoms in the $|\{1s2s\}^3S_1\ M=1\rangle$ state diffract from a polarization gradient light field formed by counterpropagating σ^+ and σ^- polarized laser beams in the presence of a homogeneous magnetic field. In the near-adiabatic regime, energy conservation allows the resonant exchange between magnetic energy and kinetic energy. As a consequence, symmetric diffraction of $|M=0\rangle$ or $|M=-1\rangle$ atoms in a single order is achieved, where the order can be chosen freely by tuning the magnetic field. We present experimental results up to sixth-order diffraction ($24\hbar k$ momentum splitting, i.e., 2.21 m/s in transverse velocity) and present a simple theoretical model that stresses the similarity with conventional Bragg scattering. The resulting device constitutes a flexible, adjustable, large-angle, three-way coherent atomic beam splitter with many potential applications in atom optics and atom interferometry.

I. INTRODUCTION

Coherent beam splitters form an essential element of atom interferometers. One way to construct such an atomic beam splitter is Bragg scattering, where atoms are diffracted by a standing light wave. The atoms are partially transmitted (zero-order diffraction) and partially diffracted into a single order, corresponding to specular reflection of the incoming atoms from the wave fronts of the light. These Bragg beam splitters have been used successfully to construct Mach-Zehnder-type atom interferometers [1,2].

Diffraction of the atoms can be viewed as resulting from the subsequent absorption and stimulated emission of photons from the left and right running components of the standing light wave. This results in an atomic momentum change of even multiples of the photon recoil momentum. The restriction to transmission or reflection can be understood in terms of energy conservation. With the axial velocity of the atoms much larger than the transverse velocity, the system can be reduced to a one-dimensional problem. If the interaction lasts long enough and the switching as determined by the laser profile and the axial velocity is sufficiently gradual, the process develops adiabatically. Energy conservation then requires the square of the transverse momentum to be conserved. Atomic Bragg scattering has been studied extensively [3–7]. In previous work [8], we achieved clean, single-order diffraction up to eighth order. With ultracold cesium atoms, interferometry with Bragg beam splitting up to 12th order has been demonstrated recently [9].

Here, we report on a unique atomic beam splitter. It combines the advantages of standard Bragg scattering (adiabatic transfer into a single, very high diffraction order) with the convenience of tuning the splitting angle by simply tuning a magnetic field instead of mechanically adjusting the angle between laser beam and atomic beam. It also offers the added flexibility of a three-port beam splitter.

II. QUASI-BRAGG-SCATTERING

The experimental configuration uses counterpropagating σ^+ and σ^- light beams to create a quasistanding light wave (with strong polarization gradient but no intensity modulation) and a homogeneous, orthogonal magnetic field. The incoming $J=1$ metastable helium atoms intersect the light wave perpendicularly. The waist of the Gaussian light wave along the axial direction of the atomic beam and the light intensity are such that the interaction is well outside the Raman-Nath regime. Although the effective light shift potentials are much deeper than the recoil energy and we are thus outside the Bragg regime, the interaction develops smoothly enough for adiabatic following of instantaneous eigenstates to play a dominant role [10,11]. This forms a clear distinction with the experiments of Ref. [12], which are performed in the Raman-Nath regime [13].

In our configuration the initial transverse momentum of the atoms is zero. Thus, the square of the transverse momentum cannot be conserved in diffraction. Furthermore, the polarization configuration does not lead to a light shift grating for a two-level system. Both effects suppress conventional Bragg scattering. However, efficient diffraction can still occur through a mechanism we call quasi-Bragg-scattering [14]. This process is best described by a two-step cycle in a reference frame with the main quantization axis along the **k** vectors of the light. First, absorption of a σ^- photon from one laser beam followed by stimulated emission of a σ^+ photon into the other laser beam transfers the atom from the $|M=+1\rangle$ state to the $|M=-1\rangle$ state, while changing the momentum of the atom by $2\hbar k$. Here, M is the magnetic quantum number of the atom and $k=2\pi/\lambda$ is the wave number of the light with λ as the wavelength of the light. In the second step, Larmor precession in the transverse magnetic field rotates the atoms via the $|M=0\rangle$ state back to the $|M=1\rangle$ state, completing the cycle.

Without magnetic field, the atoms can only return from $|M=-1\rangle$ to $|M=+1\rangle$ by returning the momentum gained in the first step to the light field, effectively undoing the diffraction process. Therefore, this description emphasizes a funda-
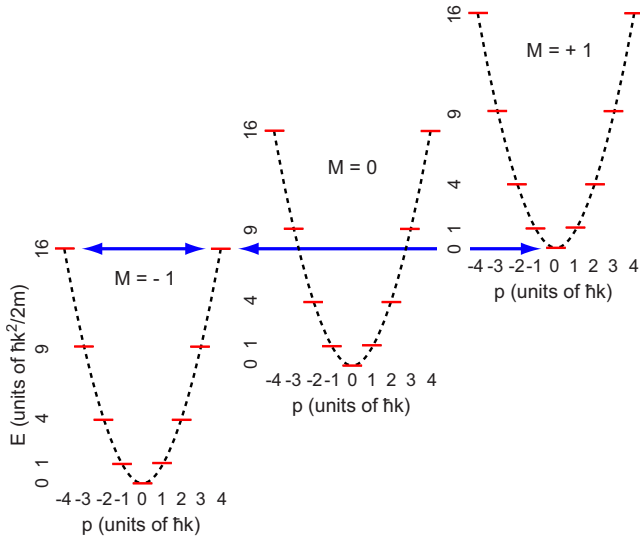
*k.a.h.v.leeuwen@tue.nl

FIG. 1. (Color online) Quadratic kinetic-energy potentials $E_{\text{kin}} = p^2/2m$ for the three magnetic substates in a $J=1$ system. In a magnetic field the energy levels of the substates are no longer degenerate but shifted by the Zeeman interaction ($\Delta E = g_L m \mu_B B$). For quasi-Bragg-diffraction the magnetic field is tuned to balance the increase in transverse kinetic energy. In the figure, the resonance between the $|M=1, p=0\hbar k\rangle$ state and the $|M=-1, p=\pm 4\hbar k\rangle$ state is indicated by the arrows.

FIG. 2. (Color online) Double Stern-Gerlach deflection "tags" each atom according to its initial and final magnetic substates. Diffraction patterns emerge horizontally, perpendicular to the magnetic deflection.

mental difference from standard Bragg scattering: without the presence of the transverse magnetic field scattering above first order is prohibited, even in the Raman-Nath regime.

Alternatively, we can also describe the process in a reference frame with the quantization axis along the magnetic field. In this frame, the energy conservation criterion is illustrated in Fig. 1. The magnetic sublevels are now nondegenerate. Outside the Raman-Nath regime, the kinetic energy cannot be neglected. Therefore we must add to each magnetic substate the kinetic energy term which is quadratic in the transverse momentum p. For particular values of the magnetic field we can create degeneracy between Zeeman levels with different transverse kinetic energies. The light field, in this reference frame a superposition of σ^+, σ^-, and π polarizations, then effectively couples these degenerate eigenstates through multiphoton Raman transitions.

Efficient transfer to a single diffraction order can now be achieved, e.g., by starting with atoms in the $|M=1, p=0\hbar k\rangle$ substate and tuning the magnetic field such that its energy equals the kinetic energy of the diffracted states $|M=-1, p = \pm 2n\hbar k\rangle$ with n as the diffraction order.

III. EXPERIMENTAL SETUP

In this work, we demonstrate magnetically induced quasi-Bragg-diffraction experimentally. In our setup we produce a monochromatic, bright, and well-collimated beam of metastable helium atoms. The beam is collimated by two-dimensional (2D) laser cooling, slowed in a Zeeman slower to 247 ± 4 m/s, prefocused by a magneto-optic lens, and compressed by a magneto-optic funnel. The design of the beam setup is described elsewhere [15]. After the compres-
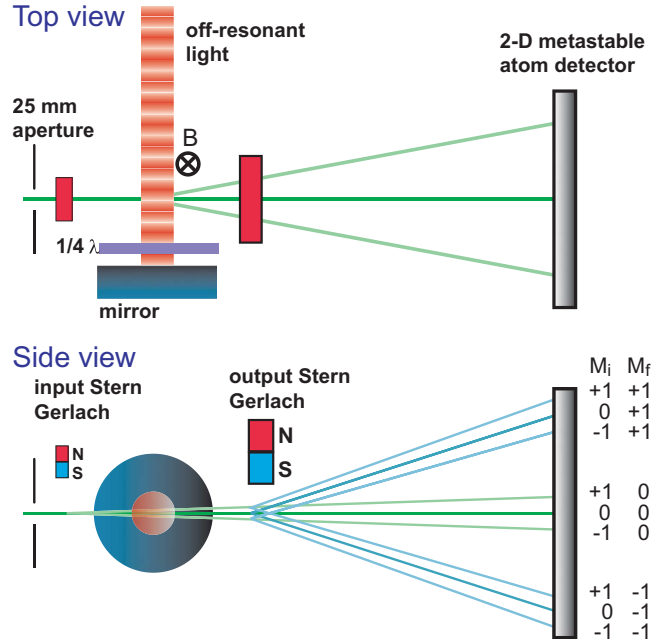
sion stage, the beam passes a 25-μm-diameter aperture 2 m downstream. We obtain a flux of 250 atoms per second in the metastable triplet $^3S_1$ state after the aperture with a transverse velocity spread of 0.05 m/s. In the experiments described below, approximately 75% of the atoms are in the $M=1$ state.

After the collimation aperture the two counterpropagating laser beams (1.6 mm waist radius) with opposite circular polarization intersect the atomic beam. Typically, the laser frequency is detuned 1 GHz above the resonance with the $\{1s2s\}^3S_1$-to-$\{1s2p\}^3P_2$ transition at 1083 nm to prevent population of the excited state and subsequent decay. A set of Helmholtz coils enables nulling of the ambient magnetic field and application of the desired homogeneous magnetic field at the interaction region (typically less than 1 G).

Diffraction of the atoms by the light occurs in the horizontal plane. The horizontal position of the atom on the 2D position-sensitive detector 2 m downstream of the interaction region gives the final momentum state of the atom after the quasi-Bragg-diffraction process.

As quasi-Bragg-scattering involves the transition between two specific magnetic substates, we need a diagnostic tool that can select and resolve the atom's magnetic state before and after the interaction. This is achieved by also mapping the magnetic information onto position information by including Stern-Gerlach regions with inhomogeneous magnetic fields (see Fig. 2). These fields are produced by small permanent magnets. The first magnet is positioned in front of the interaction region with the light. The gradient of the magnetic field is vertical. For metastable helium atoms in the triplet $^3S_1$ state, this results in three distinct vertical positions on the position-sensitive detector, enabling identification of
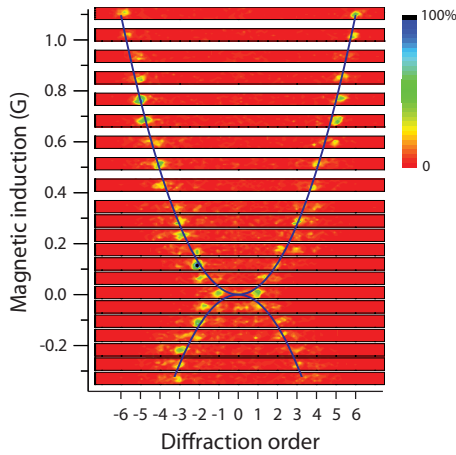
FIG. 3. (Color online) High-order quasi-Bragg-diffraction as a function of applied magnetic field. The spin-polarized beam was prepared in the $|M=1\rangle$ state with zero transverse momentum. As the magnetic field is stepwise increased, the detected diffraction patterns for atoms in the $|M=-1\rangle$ output state are displayed. The vertical position of each of the detector images is centered on its magnetic field value. At each field strength, the diffraction pattern shows primarily scattering to one particular order (plus its mirrored order) that is closest to an energy resonance as illustrated in Fig. 1. This is demonstrated by the solid line (double parabola), which indicates the exact energy resonance. The highest diffraction order observed (6, corresponding to $24\hbar k$ momentum splitting between the beams) is only limited by the finite dimensions of the detector. A small fraction of the atoms, primarily at low magnetic field, is scattered to other diffraction orders. Approximately 20% of the atoms undergo spontaneous emission at the laser power and detuning used.

double parabola (solid line) indicates where the magnetic energy balances the gain in kinetic energy.

the atom's initial Zeeman substate. The separation of the trajectories at the position of the laser beams is very small compared to the laser waist. Similarly, a second (stronger) Stern-Gerlach magnet after the interaction region separates the atoms vertically according to the Zeeman substate after the interaction. The position of each atom on the detector thus completely identifies the initial and final $|M,p\rangle$ states, providing a complete characterization of the diffraction process.

IV. RESULTS

In the first series of measurements the magnetic field is increased in small steps while the laser intensity is kept constant at 51 mW. The laser frequency is kept at a detuning $\Delta=1.3$ GHz. We select those atoms from the data that are initially in the $|M=+1\rangle$ input state and end up in the $|M=-1\rangle$ output state, as well as the atoms that end up in the $|M=0\rangle$ state. Figure 3 presents the results of 21 measurements of the $|M=+1\rangle\rightarrow|M=-1\rangle$ atoms. The vertical position of each of the detector images is centered on its magnetic field value. At each field strength, the diffraction pattern shows primarily scattering to one particular order (plus its mirrored order) that is closest to an energy resonance as illustrated in Fig. 1. This is demonstrated by the solid line (double parabola), which indicates the exact energy resonance. The highest diffraction order observed (6, corresponding to $24\hbar k$ momentum splitting between the beams) is only limited by the finite dimensions of the detector. A small fraction of the atoms, primarily at low magnetic field, is scattered to other diffraction orders. Approximately 20% of the atoms undergo spontaneous emission at the laser power and detuning used.

From the full set of measurements, the field strengths at which the transfer is most efficient have been determined for each diffraction order. The results for both the $|M=+1\rangle$
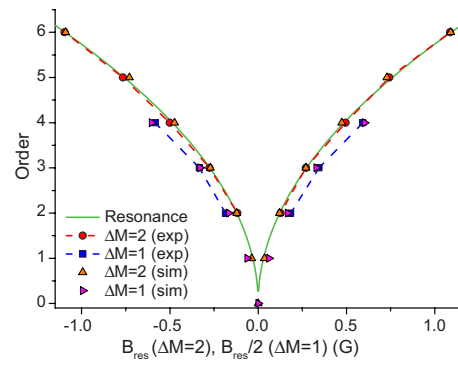

FIG. 4. (Color online) Optimal magnetic field for each observed diffraction order for atoms transferred from $|M=1\rangle$ to $|M=-1\rangle$ ($\Delta M=2$) as well as for those transferred from $|M=1\rangle$ to $|M=0\rangle$ ($\Delta M=1$). The experimental data points are connected by dashed lines for clarity. The drawn line indicates where the loss in magnetic energy balances the gain in kinetic energy. The triangles are the result of numerical simulations. The overall calibration factors of the magnetic field and of the laser intensity in the presented data are adjusted for best fit between data and simulation. The optimum values (fixed for all measurements) are equal to independently measured values to well within the estimated 10% uncertainty interval in the latter.

$\rightarrow|M=-1\rangle$ and the $|M=+1\rangle\rightarrow|M=0\rangle$ atoms are plotted in Fig. 4. Both sets of data agree very well with the results of simulations (indicated by the triangles in the figure). These simulations are based on direct numerical integration of a time-dependent Schrödinger equation. The quasi-Hamiltonian used includes the kinetic energy of the atom and the interaction with the Gaussian-shaped light field, as well as a damping term accounting for the loss by spontaneous emission. The divergence of the incoming atomic beam is also taken into account in the simulations.

Figure 4 shows that the $|M=+1\rangle\rightarrow|M=-1\rangle$ results are very close to the expected resonance (solid line), whereas the $|M=+1\rangle\rightarrow|M=0\rangle$ results deviate by 20%–50% from the resonant B field. These deviations are an indication that quasi-Bragg-scattering is not quite as simple as the basic adiabatic description given earlier. Detailed analysis shows that in fact quasi-Bragg-scattering is not allowed in the fully adiabatic limit. Transfer occurs by nonadiabatic Landau-Zener-type transfer near anticrossings of input and output states that are initially close in energy, but not degenerate. This mechanism, similar to the off-resonant Bragg scattering studied in an earlier paper [16] and discussed also by Muller *et al.* [11], will be discussed in a forthcoming paper.

In a second set of measurements the power dependence of the $|M=1\rangle$-to-$|M=0\rangle$ transition was investigated. Figure 5 shows the results. The magnetic field is kept fixed at resonance for fourth-order diffraction $[g_L\mu_B B=(8\hbar k)^2/2M_a =1.10$ G with g_L the Landé factor and M_a the atomic mass] and the detuning at $\Delta=1.0$ GHz. The experiments (squares) and simulations, given by the solid line, are in fair agreement. The results confirm that the scattered fraction exhibits an oscillatory behavior similar to the Pendellösung oscillations in Bragg scattering. The small amplitude of the first maximum of the oscillation in the simulations is a consequence of the nonadiabatic character of the $|M=1\rangle$-to-$|M=0\rangle$ transition.
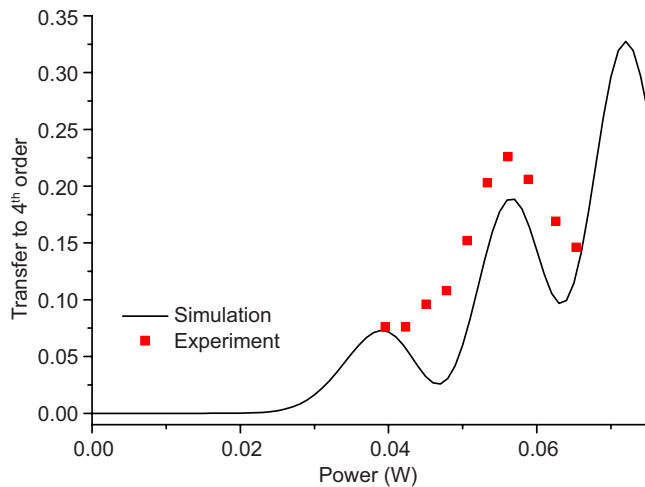
FIG. 5. (Color online) Efficiency of fourth-order $|M=1\rangle$-to-$|M=0\rangle$ quasi-Bragg-diffraction versus laser power.

The maximum overall efficiency achieved in this series of quasi-Bragg-experiments is 30%. Although this is already quite acceptable for many applications of a large-angle atom beam splitting, further improvement can be easily realized. The limited efficiency is attributable for a large part to the divergence of the atomic beam ($0.6\hbar k$, whereas the width of the resonance corresponds to $0.25\hbar k$). The divergence was chosen quite large compared to our earlier experiments on regular Bragg scattering [8] in order to allow for quick scans of the parameter space. For a smaller part, the efficiency is limited by residual spontaneous emission, reducing the co-

herently diffracted population. Our simulations show that these issues can be solved by reducing the divergence of the atom beam by a factor of 2 and by optimizing the intensity and detuning of the laser. In this way a diffraction efficiency of 90% can be readily achieved.

V. CONCLUSIONS

To summarize our results we have demonstrated that clean, high-order atomic diffraction can be achieved in the presence of a $\sigma^+\sigma^-$ polarized light field and an orthogonal magnetic field. This quasi-Bragg-diffraction is based an effi-cient and coherent scattering process in which magnetic en-ergy is converted to kinetic energy. The order of the (sym-metric) diffraction is fully determined by the amplitude of the magnetic field, obviating the need for mechanical adjust-ments of the laser-to-atom angle. The scattering process in-herently alters the magnetic substate, which can be advanta-geous for high-precision applications (atom interferometry) where it may be easier to produce a spin-polarized $|M=\pm 1\rangle$ input beam but desirable to have an $|M=0\rangle$ state dur-ing the measurements, as this state is to first order insensitive to stray magnetic fields. The population of the diffracted or-der displays an oscillatory behavior as a function of laser intensity, analogous to the Pendellösung oscillation in con-ventional Bragg diffraction.

[1] D. M. Giltner, R. W. McGowan, and S. A. Lee, Phys. Rev. Lett. **75**, 2638 (1995).

[2] Y. Torii, Y. Suzuki, M. Kozuma, T. Sugiura, T. Kuga, L. Deng, and E. W. Hagley, Phys. Rev. A **61**, 041602(R) (2000).

[3] P. J. Martin, B. G. Oldaker, A. H. Miklich, and D. E. Pritchard, Phys. Rev. Lett. **60**, 515 (1988).

[4] D. M. Giltner, R. W. McGowan, and S. A. Lee, Phys. Rev. A **52**, 3966 (1995).

[5] M. K. Oberthaler, R. Abfalterer, S. Bernet, J. Schmiedmayer, and A. Zeilinger, Phys. Rev. Lett. **77**, 4980 (1996).

[6] S. Dürr, S. Kunze, and G. Rempe, Quantum Semiclassic. Opt. **8**, 531 (1996).

[7] S. Dürr and G. Rempe, Phys. Rev. A **59**, 1495 (1999).

[8] A. E. A. Koolen, G. T. Jansen, K. F. E. M. Domen, H. C. W. Beijerinck, and K. A. H. van Leeuwen, Phys. Rev. A **65**, 041601(R) (2002).

[9] H. Muller, S. W. Chiow, Q. Long, S. Herrmann, and S. Chu, Phys. Rev. Lett. **100**, 180405 (2008).

[10] C. Keller, J. Schmiedmayer, A. Zeilinger, T. Nonn, S. Dürr, and G. Rempe, Appl. Phys. B: Lasers Opt. **69**, 303 (1999).

[11] H. Muller, S. W. Chiow, and S. Chu, Phys. Rev. A **77**, 023609 (2008).

[12] T. Pfau, C. Kurtsiefer, C. S. Adams, M. Sigel, and J. Mlynek, Phys. Rev. Lett. **71**, 3427 (1993).

[13] B. Dubetsky and P. R. Berman, Phys. Rev. A **64**, 063612 (2001).

[14] The name "quasi-Bragg-scattering" is based on the shared characteristics with regular Bragg scattering: population of a single diffraction order due to (approximate) energy conserva-tion. It is used in a more general sense than in Ref. [11], where it refers to the transition regime between resonant Bragg and nonresonant Raman-Nath diffractions.

[15] R. M. S. Knops, A. E. A. Koolen, H. C. W. Beijerinck, and K. A. H. van Leeuwen, Laser Phys. **9**, 286 (1999).

[16] M. A. H. M. Jansen, K. F. E. M. Domen, H. C. W. Beijerinck, and K. A. H. van Leeuwen, Phys. Rev. A **76**, 053629 (2007).